energies

Article

Evaluation of Thermal-Physical Properties of Novel Multicomponent Molten Nitrate Salts for Heat Transfer and Storage

Na Li, Yang Wang, Qi Liu and Hao Peng *

Shanghai Institute of Applied Physics, Chinese Academy of Sciences, Shanghai 201800, China
* Correspondence: penghao@sinap.ac.cn; Tel.: +86-021-39194053

Abstract: In this work, a novel eutectic nitrate molten salt mixture of the $NaNO_3$-KNO_3-$Ca(NO_3)_2$ (16:48:36 wt%) ternary system with the significant advantage of low melting temperature was successfully designed and prepared using the static fusion method. Then, its thermal-physical properties, such as the melting point, fusion enthalpy, thermal stability, specific heat capacity, thermal diffusivity, thermal conductivity, density, and viscosity, were respectively measured by a modified or self-developed experimental device. Meanwhile, for better understanding and evaluating the heat transfer and storage performances of the material, the thermal-physical properties of this studied molten salt were further compared with those of other currently potential nitrate/nitrite systems in concentrating solar power (CSP) applications. The results proved that the newly developed $NaNO_3$-KNO_3-$Ca(NO_3)_2$ system has excellent thermal-physical properties and flow characteristics. Moreover, the cost analysis also showed the new salt has good economic performance with potential market competitiveness, its price is determined to be only 42.48 ¥/kg. All of these advantages make it a promising candidate material for heat transfer fluid (HTF) and thermal energy storage (TES) in CSP applications. This work is useful and significant for developing new molten salt materials and choosing appropriate media of HTF and TES in CSP plants or other probable thermal power generation facilities.

Keywords: novel molten nitrate salt; heat transfer fluid (HTF); thermal energy storage (TES); thermal-physical properties; concentrating solar power (CSP)

Citation: Li, N.; Wang, Y.; Liu, Q.; Peng, H. Evaluation of Thermal-Physical Properties of Novel Multicomponent Molten Nitrate Salts for Heat Transfer and Storage. *Energies* **2022**, *15*, 6591. https://doi.org/10.3390/en15186591

Academic Editor: Edward Halawa

Received: 5 August 2022
Accepted: 6 September 2022
Published: 8 September 2022

1. Introduction

In recent years, with the massive consumption of fossil fuels, such as coal, oil, and natural gas, these non-renewable energy sources are gradually depleting toward exhaustion. Moreover, the emission of carbon dioxide gas from fossil fuels into the environment has markedly increased. Carbon dioxide, which is a greenhouse gas, is recognized as the most important factor in global warming [1–3]. Therefore, vigorously developing green and clean renewable energy, such as solar and wind energy, is imperative and urgent. The wide application of these environmentally friendly energy sources will introduce considerable changes to the current energy structure.

Concentrating solar power (CSP) is a kind of technology that concentrates the heat of sunlight to generate electricity. However, the intermittency effect of solar energy radiation is harmful to the steady and equilibrated energy supply and demand. Hence, thermal energy storage (TES) plays a vital role in improving the utilization efficiency of renewable energy [4,5]. The TES material is responsible for effective thermal management in CSP and can provide a certain number of hours of extended heating transfer to reduce radiation mismatch in time and space and resolve the problem of strong mismatch between energy supply and user demand [6,7]. In addition, the use of TES materials can reduce energy wastage and increase the energy conversion efficiency of process systems.

A TES system requires a transfer-thermal storage fluid that can operate at high temperatures with a low vapor pressure and a high energy capacity to transfer heat from the solar receiver to the target heat exchanger effectively. Recently, different types of materials, especially inorganic salts, have been extensively investigated for potential use in heat collection and storage [2,8–10].

Using mixed molten salts as heat transfer and storage fluid is one of the three core technologies of solar thermal power generation. The mixed nitrate molten salts have the advantages of low melting point, large specific heat capacity, good thermal conductivity, low viscosity, low vapor pressure, and low corrosiveness to metal materials. Owing to these advantages, nitrate salt mixtures become the most general and important heat transfer and storage materials in CSP plants [11], which have been widely used in industrial applications.

Binary nitrate mixtures of Solar Salt, which comprises 60 wt% $NaNO_3$ + 40 wt% KNO_3 with a melting point of 240 °C, are frequently utilized as sensible heat storage media in commercial CSP plants [12–15]. Moreover, the ternary reciprocal Hitec system ($NaNO_3$-KNO_3-$NaNO_2$) and the $NaNO_3$-KNO_3-$LiNO_3$ systems are extensively used molten salt mixtures for CSP plants [16–18]. The composition of the minimum melting point of Hitec is usually reported as $NaNO_3$-KNO_3-$NaNO_2$ (7-53-40 wt%) with a melting temperature of 142 °C [19]. The melting points of Solar Salt and Hitec are satisfactorily low; however, the low stabilities of these systems at high temperatures limit their working temperature range. The low thermal stability is a common defect for most nitrate/nitrite systems, which generally confines their maximum operating temperature to less than 600 °C. Compared with nitrates, molten chloride salts have thermophysical advantages associated with their high operating temperatures in CSP dish and tower applications [20,21]; thus, molten chloride salts have been regarded as potential heat transfer fluids (HTF) and TES media in the generation III CSP (GIII-CSP) field due to their relatively good thermal stabilities [20,22–25].

The recommended working temperature by the SunShot plan for GIII-CSP plants was 550 °C–750 °C [26–28]. The SunShot initiative focuses on the application of molten chloride systems NaCl-KCl-$ZnCl_2$ (7.5 wt%–23.9 wt%–68.6 wt%) and KCl-$MgCl_2$ (62.5 wt%–37.5 wt%) as advanced TES/HTF media in GIII-CSP plants [29]; when combined with alkali metal chlorides, the divalent metal ions (Mg^{2+} and Zn^{2+}) can decrease the melting points below 400 °C and increase the thermal stabilities up to 800 °C [30,31].

However, the slightly attractive cost and high corrosiveness of chloride salts relative to nitrates limit their industrial scale and demand. Moreover, the commercial application of chloride mixtures is limited due to their relatively high melting points and low specific heat capacities, which will require additional equipment maintenance during cold seasons and occupy a large space. The thermal stability of chloride salts is generally higher than that of nitrate mixtures. However, the relatively high melting point of chlorides generally narrows their operating temperature range. Therefore, attention should be focused on the design and development of new multicomponent nitrate systems with optimized performances. Thus, a comprehensive evaluation of the thermophysical properties of these new materials is a key work.

The latest generation of currently commercialized nitrate salts is Hitec XL ($NaNO_3$-KNO_3-$Ca(NO_3)_2$) and its operating temperature window is 393–773 K. However, Gaune et al. [32] and Gomez et al. [33] reported that the composition of the eutectic point and the melting point of this ternary system are not in consistent with each other, and data in some other pieces of literature even substantially differ. Therefore, accurately finding the composition of the eutectic point of the ternary $NaNO_3$-KNO_3-$Ca(NO_3)_2$ system and further estimating its corresponding thermophysical properties is meaningful work.

A eutectic nitrate molten salt of the $NaNO_3$-KNO_3-$Ca(NO_3)_2$ (16:48:36 wt%) ternary system with low melting temperature of 382.1 K was successfully designed and prepared in this work using the static fusion method. The thermophysical properties of this newly developed material were then experimentally characterized. Meanwhile, the thermophysical properties of the $NaNO_3$-KNO_3-$Ca(NO_3)_2$ (16-48-36 wt%) were compared with other commonly used nitrate/nitrite salts. The results showed that the system has excellent

thermal-physical properties, including suitable phase change temperature, high heat capacity, good thermal conductivity, acceptable thermal stability, and wide working temperature range. Particularly, a quite low melting point is a remarkable improvement and may be the largest advantage for this novel system. The system also has good fluid properties with suitable density and low viscosity. In addition, this system has good economic performance with attractive cost. Thus, this salt becomes a potential candidate TES/HTF material in CSP plants with high efficiency supercritical CO2 (S-CO2) cycles due to the aforementioned advantages. Meanwhile, this material may also be used in other probable thermal power-generation facilities.

2. Materials and Methods

2.1. Eutectic Salt Preparation

High-purity $NaNO_3$, KNO_3, and $Ca(NO_3)_2{\cdot}4H_2O$ were supplied by Sinopharm Chemical Regent Co., Ltd. The purity of all these salts was more than 99.9%. $NaNO_3$ and KNO_3 powdery salt were placed in a quartz crucible and separately dried at 473 K under dry ultrapure argon (Ar; 99.999%) atmosphere for 24 h to facilitate dehydration. $Ca(NO_3)_2{\cdot}4H_2O$ was heated in an electric furnace to 473 K and maintained at this temperature for 72 h, and then it was heated to 573 K and maintained at this temperature for 72 h to dehydrate. $Ca(NO_3)_2{\cdot}4H_2O$ will lose its crystal water in this process and form the anhydrous $Ca(NO_3)_2$. The three single-treated salts were then accurately weighed and fully blended in accordance with the designed proportion ($NaNO_3$-KNO_3-$Ca(NO_3)_2$ = 16:48:36 wt%) under an Ar atmosphere condition. The mixed salts were transferred to an electric furnace and heated to 523 K for approximately 30 min and maintained at this temperature for 48 h. The mixture sample was then naturally cooled to the ambient temperature and preserved in a glove box for subsequent experiments. The moisture and oxygen concentrations in the glove box atmosphere were strictly controlled below 0.5 ppm. Trace impurities in the prepared molten salt samples will not influence the experimental measurements and results.

2.2. Characterization Method and Analysis Device

The melting point and fusion enthalpy of the $NaNO_3$-KNO_3-$Ca(NO_3)_2$ eutectic salts were measured by a differential scanning calorimeter (DSC, NETZSCH DSC-404 F3), as shown in Figure 1. The device was calibrated by four certified reference materials, namely In, Bi, Sn, and Zn metals, in the temperature range of 373 K–1273 K before measurement of $NaNO_3$-KNO_3-$Ca(NO_3)_2$ eutectic salts. The samples (ca. 10.0 mg) were added into the test pan and then heated from ambient temperature up to 473 K under Ar atmosphere. Calibration and measurement were completed under Ar atmosphere flowing with 50 mL/min at the heating rate of 10.0 K/min. The measurement processes were repeated thrice to ensure the accuracy and reproducibility of the experimental results. Temperature and heat measurement errors are important sources of DSC uncertainty, mainly including reference material constant, sample weighing, measurement reproducibility, ambient temperature, etc. The uncertainty of temperature measurement by DSC was estimated to be $\pm$1.0 K, and the uncertainty of fusion enthalpy was estimated to be around $\pm$2%.

The thermal stability of the salt sample was analyzed by a thermogravimetric analyzer (TGA, SteramLabsys Evo), as shown in Figure 2. The empty graphite testing crucible was first heated to 823 K as the blank result. The heating rate was 10.0 K/min under Ar atmosphere. The salt sample (29.7 mg) was then placed in the crucible after the blank test and heated to 823 K under the same conditions. The main sources of uncertainty in thermogravimetric analysis include the balance sensitivity, material and shape of the crucible, property and mass of the sample, type of atmosphere and flow rate, and baseline drift, etc. In present study, the uncertainty of the thermal stability measurement was estimated below 2 K.

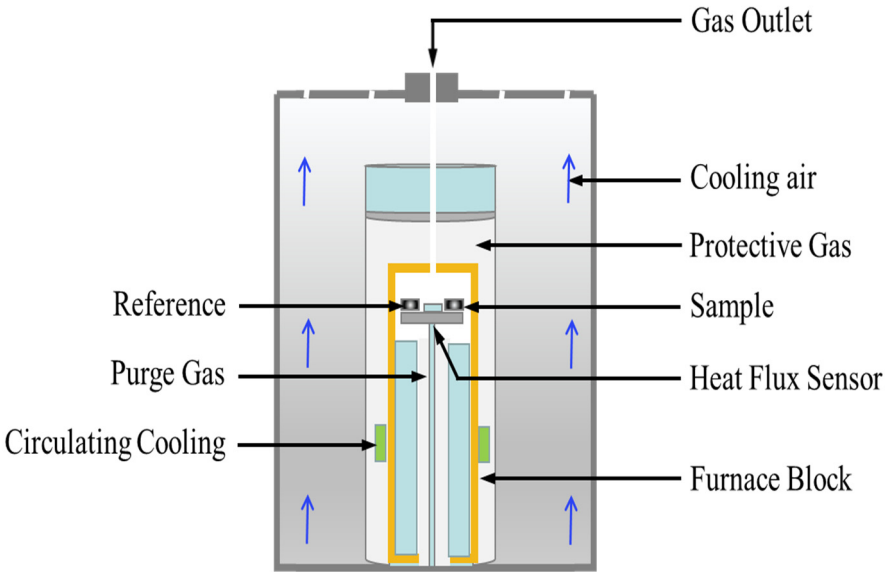

Figure 1. Schematic of the differential scanning calorimeter setup for melting point, fusion enthalpy, and specific heat capacity measurements.

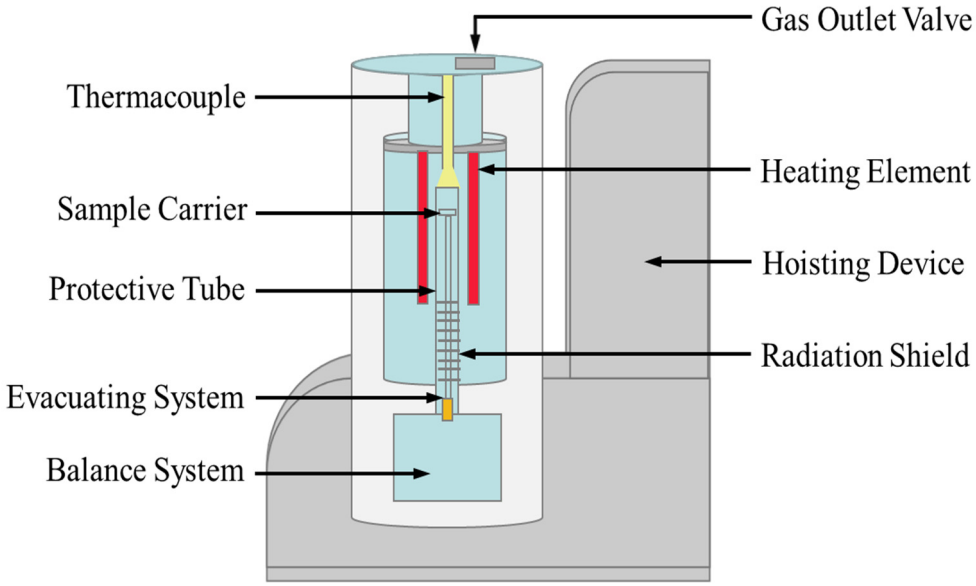

Figure 2. Schematic of the thermogravimetric analyzer for thermal stability measurement.

The specific heat capacity of the $NaNO_3$-KNO_3-$Ca(NO_3)_2$ eutectic salt was also determined using the heat capacity ratio method by DSC under Ar atmosphere at a heating rate of 10.0 K/min (Figure 1). The empty graphite testing crucible was first heated to 773 K as the baseline. A standard material of sapphire was then placed into the crucible and heated as reference sample. The $NaNO_3$-KNO_3-$Ca(NO_3)_2$ samples (ca. 40.0 mg) were finally measured under the same conditions. The detailed measurement process of specific heat capacity was described in previous studies [34]. The major sources of uncertainty are the repeatability of the blank measurement (two empty crucibles), specific heat capacity of reference sample, heating rate, and sample mass. In the present study, the uncertainty of the specific heat capacity was estimated to be 0.08 J/g·K [35].

Density measurements of the $NaNO_3$-KNO_3-$Ca(NO_3)_2$ molten salts were realized by a device constructed on the basis of Archimedes theory, as shown in Figure 3. The device was calibrated by pure NaCl [36]. The usage standards of the crucible, platinum cylinder, and platinum wire are specified, and their dimensions are also strictly regulated and fixed.

The effect of surface tension on the total error (<0.2%) and uncertainty are sufficiently small and negligible, which can be ignored in density measurements [37,38]. The volume of the platinum cylinder was calibrated by distilled water at ambient temperature before measuring the density of molten nitrate salts. Approximately 300 g of molten nitrate salt powdery sample was melted at target temperature in a furnace with Ar atmosphere protection. The platinum cylinder, which is connected to an electronic balance through a platinum wire, was completely dipped and immersed into the molten salt, and the electronic balance values were recorded at desired temperatures during the cooling process at the rate of 1 K/min. The density is calculated in accordance with Equation (1). The major sources of uncertainty are accuracy of volume measurements of platinum cylinder ($<2 \times 10^{-4}$ cm^3), accuracy of the balance (0.1 mg), and determination of temperature ($\pm$1 K). In present study, the uncertainty of density was estimated to be less than 0.0039 g/cm^3 [36].

$$\rho = \frac{m_1 - m_2 + \pi D\sigma/g}{V_0[1 + \beta(T - 298)]^3} \quad (1)$$

where ρ is the density, V_0 is the weight and volume of the platinum cylinder in air, m_1 and m_2 are the weights of the platinum cylinder in distilled water and molten salts, respectively, σ is the surface tension of molten salts, D is the diameter of platinum wire (D = 0.2 mm), g is the gravitational constant, T (K) is the temperature of molten salts, and β is the linear expansion coefficient of platinum ($\beta = 9 \times 10^{-6}$/K).

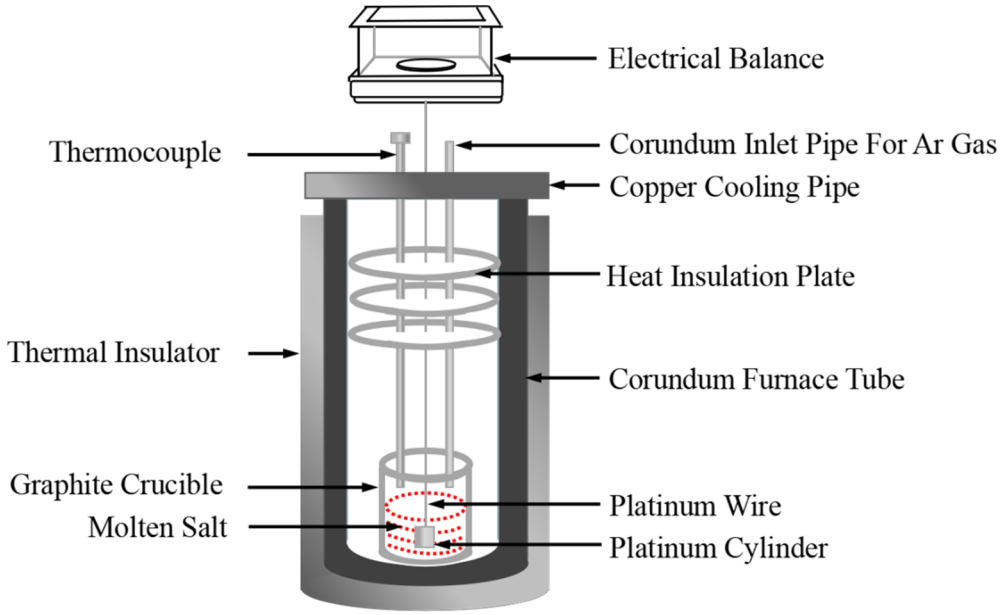

Figure 3. Schematic of the density measurement experimental setup.

Thermal diffusivity (α) was measured by the laser flash analysis (LFA) technique, as shown in Figure 4. The $NaNO_3$-KNO_3-$Ca(NO_3)_2$ powdery salt sample (ca. 2.0 g) was placed in a graphite crucible with cover from 423 K to 773 K with an interval of 10 K. The testing cell loaded with samples was then transferred to a vacuum furnace and degassed thrice. The sample was transferred to the LFA device (Linseis LFA 1000) after degasification. The thermal conductivity (λ) can be obtained through α, known density (ρ), and the obtained specific heat (C_p), and the calculation formula is presented in Equation (2). The detailed description of the sample cell, testing method, and sample preparation can be found in previous works [37]. Generally, the uncertainty of thermal conductivity measurement is supposed to be less than 15%. In present study, the uncertainty is evaluated to be

±0.023 W/(m K) [37]. The uncertainty sources are the values of specific heat capacity, density, and thermal diffusivity.

$$\lambda = \alpha \cdot \rho \cdot C_p. \quad (2)$$

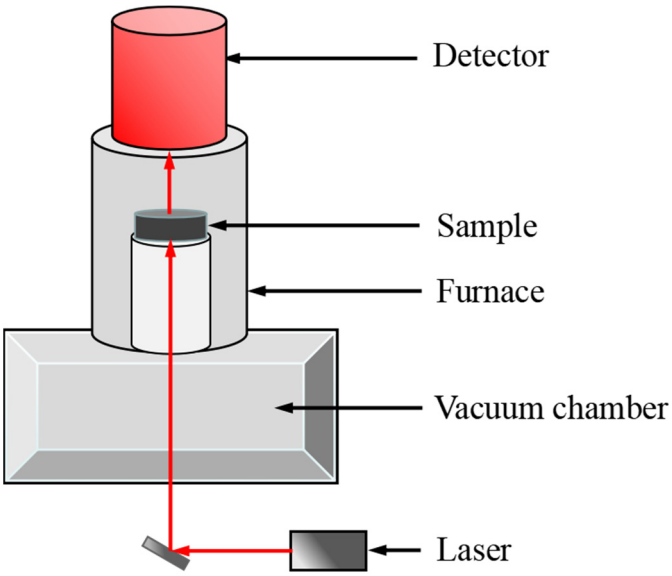

Figure 4. Schematic of LFA device for thermal diffusivity measurement.

Viscosities of the molten salts were measured by using a rotational coaxial cylinder viscometer constructed on the basis of the Brookfield DV-III-series measurement head, as shown in Figure 5. The molten nitrate salt mixtures were heated to the target temperature of 773 K and maintained at this temperature for 1 h. A K-type thermocouple was placed in the molten salt to measure its temperature accurately. The inner cylinder was driven by a motor, and the torque was recorded. The viscosity of the molten nitrate salt material can be obtained from Equation (3). The uncertainty of viscosity was estimated to be less than 2.5% [39]. The main uncertainty sources of viscometer include rotating speed, temperature, and the standard sample named S6 (a standard viscosity oil certified by NIST).

$$\eta = \frac{SMC \times Y(torque\%) \times \varepsilon \times 100}{N(rpm)}, \quad (3)$$

where η is the viscosity; $SMC = \frac{1}{4\pi(h+c)}\left(\frac{1}{r^2} - \frac{1}{R^2}\right)$ is a constant related to the dimension of crucible and rotator, and its value is calibrated by standard viscosity oil; h and r represent the length and radius of the rotator, respectively; R is the radius of the crucible; c is a constant; SMC is the calibration of standard viscosity oil; Y is the torque expressed by percentage; ε is a constant; N is the rotating speed.

It should be noted that in order to meet the needs of molten salt testing, all the instruments used in present study are modified or self-developed experimental devices. The densitometer and viscometer are completely self-developed instruments, which are designed and assembled in the laboratory, so that the two instruments can be specifically used to test molten salt samples. The LFA device for thermal diffusivity measurement is a semi-commercial instrument with modification of testing system, including crucible and sampling designs, etc. The differential scanning calorimeter (DSC) and thermogravimetric analyzer (TG) instruments were placed in a glove box and successfully avoided problems caused by the characteristic properties of molten salt samples, such as moisture absorption and surface contamination.

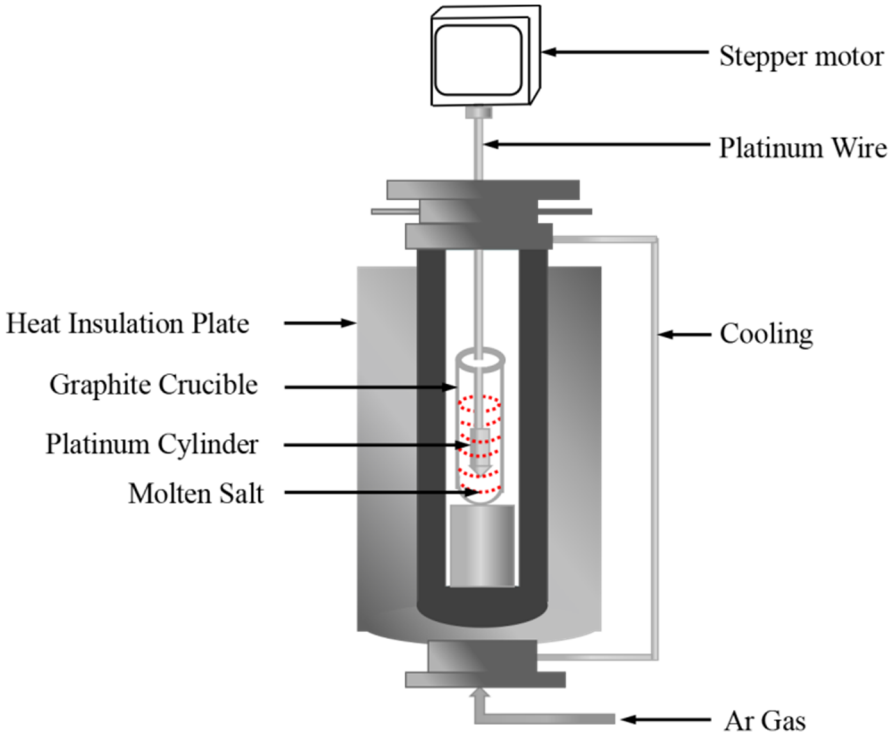

Figure 5. Schematic of the viscosity measurement method and experimental set-up.

3. Results

3.1. Melting Point and Fusion Enthalpy

The melting point is a critical parameter for evaluating the latent heat storage performance of a material. A suitable melting point can increase the heat transfer rate and decrease the charge/discharge time of the cycle, thus providing the best overall exergy efficiency for the TES systems [40,41]. The information on the melting point and the fusion enthalpy data can be obtained from the analysis of the resulting DSC curve. Figure 6 shows the obtained experimental DSC curve of the $NaNO_3$-KNO_3-$Ca(NO_3)_2$ ternary salt recorded under an Ar atmosphere with a heating rate of 10 K/min. A single melting peak can be found in the experimental DSC curve. This single peak indicates that the ternary salt is a eutectic system. The melting point of this eutectic salt can be obtained from the DSC curve, that is, the intersection of the peak's horizontal baseline and the tangent of the onset of the peak. Thus, the melting point result of the studied system was 382.1 K, as shown in Figure 6. The low melting point is a significant advantage for this system, which will be comprehensively discussed in Section 3.7. Enthalpy cannot be directly read from the DSC curve but can still be obtained by analyzing the peak signal. The enthalpy corresponds to the integration of the peak area in the DSC curve according to the DSC theory. Thus, the fusion enthalpy of the $NaNO_3$-KNO_3-$Ca(NO_3)_2$ ternary salt finally resulted in 57.9 J/g, which is consistent with the literature value of homo-system nitrates [42].

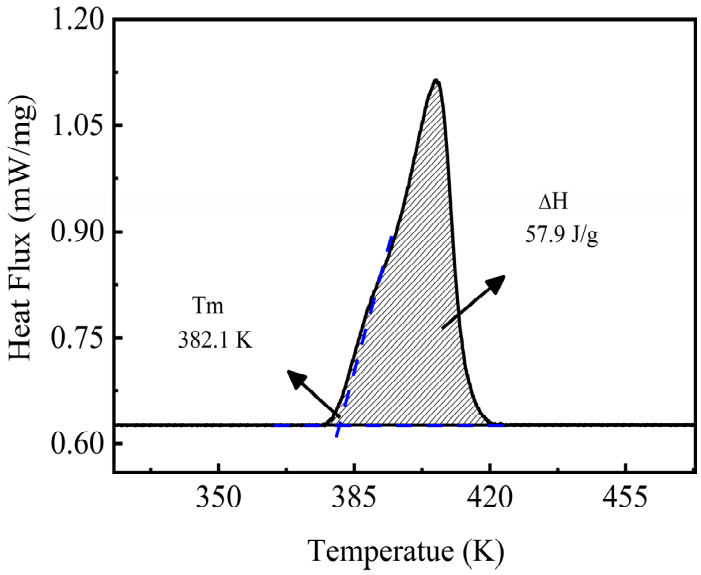

Figure 6. Melting point and fusion enthalpy of the $NaNO_3$-KNO_3-$Ca(NO_3)_2$ (16:48:36 wt%) ternary salt.

3.2. Thermal Stability

Thermal stability determined the upper limit of the working temperature of an HTF/TES medium, which corresponded to the maximum operating temperature or the decomposition temperature of molten salts. Thus, this parameter is one of the critical factors considered for material selection in high-temperature TES. Figure 7 shows the weight loss of the $NaNO_3$-KNO_3-$Ca(NO_3)_2$ ternary eutectic salt. Almost no weight change was observed before 610 K, and the weight loss began after this temperature. The weight loss between 610 K and 745 K was remarkably slow and less than 2.0%. The weight loss was still less than 3.0% even up to 771.1 K, which is defined as the decomposition temperature or the maximum operating temperature for this salt. These results suggested that the thermal stability of the $NaNO_3$-KNO_3-$Ca(NO_3)_2$ ternary eutectic salt was high with a relatively wide working temperature range. However, the thermal stability for this system was slightly lower than other currently used nitrate materials and needs to be improved (Figure 7); nevertheless, the value of 771.1 K is still acceptable and satisfactory.

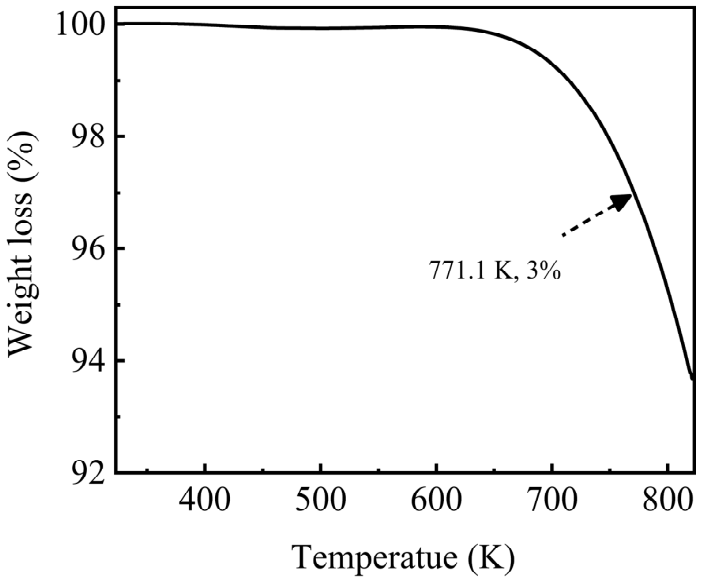

Figure 7. Weight loss of the $NaNO_3$-KNO_3-$Ca(NO_3)_2$ (16:48:36 wt%) ternary eutectic salt by TGA under Ar atmosphere from 323 K to 823 K.

3.3. Specific Heat Capacity

Specific heat capacity is also an important thermal property affecting the heat transfer and storage performance, which is an indispensable parameter for evaluating the thermal energy capacity and heat density nature of a material. The specific heat capacity in liquid state of the $NaNO_3$-KNO_3-$Ca(NO_3)_2$ ternary salt was tested from 423 K to 773 K by DSC and the results are shown in Figure 8. The specific heat capacity of the $NaNO_3$-KNO_3-$Ca(NO_3)_2$ eutectic ternary salt increased linearly with the temperature. The specific value can be fitted by a linear function of temperature ranging from 423 K to 773 K, and the relation was expressed in Equation (4). The adjusted R-square (R^2) was more than 99.97%.

$$C_p = 1.2315 + 5.3036 \times 10^{-4} T \text{ (J/g·K) } (423 \leq T \leq 773 \text{ K}). \quad (4)$$

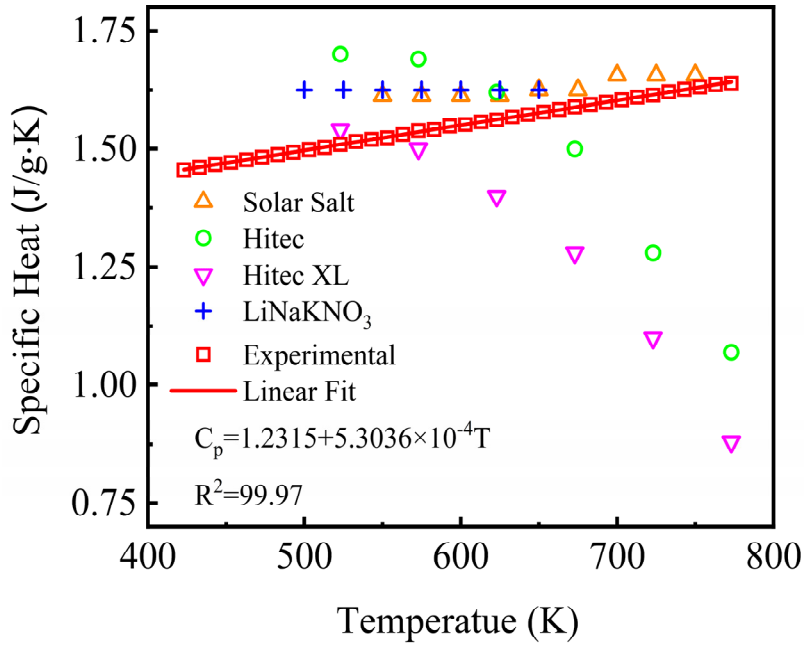

Figure 8. Specific heat capacity of the $NaNO_3$-KNO_3-$Ca(NO_3)_2$ (16:48:36 wt%) eutectic ternary salt and other currently used nitrate/nitrite systems.

The average specific heat capacity of the studied $NaNO_3$-KNO_3-$Ca(NO_3)_2$ ternary salt was obtained to be 1.55 J/g·K at the temperature range from 423 K to 773 K. Figure 8 also compared the specific heat capacity of the studied system and other nitrate salt mixtures. The average specific heat capacity of Solar Salt, Hitec, Hitec XL, and the $NaNO_3$-KNO_3-$LiNO_3$ was 1.63, 1.50, 1.33, and 1.62 J/g·K, respectively [19,34]. Comparative analysis shows that the heat capacity of the liquid state of the $NaNO_3$-KNO_3-$Ca(NO_3)_2$ ternary salt remained at a relatively high level, which was slightly higher than that of Hitec and Hitec XL and was close to that of Solar Salt and the $LiNO_3$-$NaNO_3$-KNO_3. The results indicate a relatively high thermal energy capacity and heat storage potential for this salt mixture.

3.4. Density

The density of the nitrate molten salt materials determines the volumetric heat storage density of the heat storage system, which in turn affects the heat exchange efficiency of the system. Meanwhile, obtaining accurate density is essential for the thermohydraulic calculation and safety analysis of CSP systems. Thus, density is a vital thermophysical parameter that should be acquired. The density of the $NaNO_3$-KNO_3-$Ca(NO_3)_2$ system was tested within a certain temperature range by a densitometer, which is a self-developed device constructed by the researchers of the current study based on the Archimedes principle. The density of the $NaNO_3$-KNO_3-$Ca(NO_3)_2$ was measured from 423 K to 773 K, and the experimental result was also compared with that of Solar Salt, Hitec, Hitec XL, and

the $NaNO_3$-KNO_3-$LiNO_3$ systems (Figure 9). As shown in Figure 9, the density of all five molten nitrate/nitrite salts showed negative linear relationships with temperature. The density of the $NaNO_3$-KNO_3-$Ca(NO_3)_2$ was relatively large, with a value close to Hitec XL. The specific density value can be fitted by a linear function of temperature ranging from 423 K to 773 K, as expressed in Equation (5). The adjusted R-square (R^2) was more than 99.93%. For the $NaNO_3$-KNO_3-$Ca(NO_3)_2$ ternary salt in this work, the average value of density was 1.9533 g/cm^3 within the temperature range from 423 K to 773 K.

$$\rho = 2.3605 - 6.8319T \text{ (g/cm}^3\text{)} \ (423 \leq T \leq 773 \text{ K}). \quad (5)$$

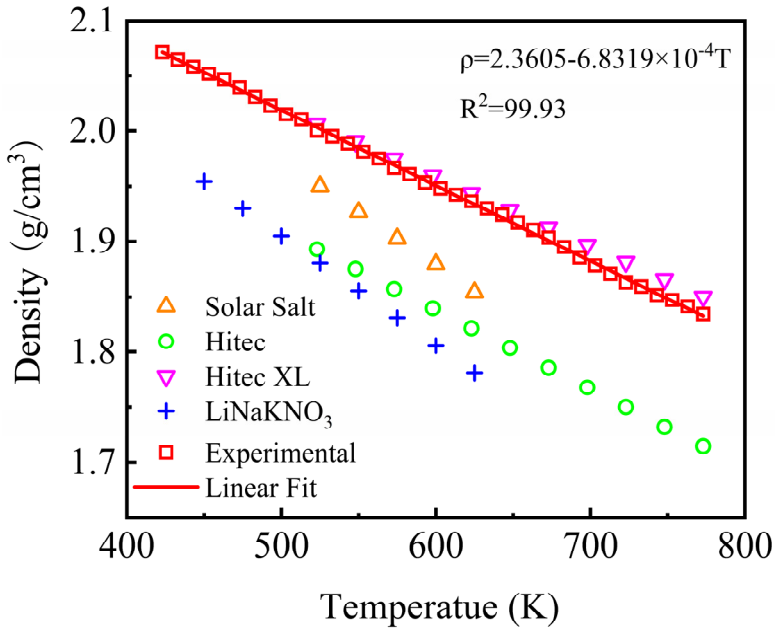

Figure 9. Densities of the $NaNO_3$-KNO_3-$Ca(NO_3)_2$ (16:48:36 wt%) eutectic ternary salt and other currently used nitrate/nitrite systems.

3.5. Thermal Conductivity

Figure 10 shows the thermal diffusivity and thermal conductivity of the $NaNO_3$-KNO_3-$Ca(NO_3)_2$ eutectic salt determined by LFA at the temperature range of 423 K to 773 K. This figure reveals that the thermal diffusivity of the $NaNO_3$-KNO_3-$Ca(NO_3)_2$ eutectic salt increased with the temperature rise, and the results were located in the range from 0.080 mm^2/s to 0.304 $\times$ 10^{-3} mm^2/s. The thermal diffusivity value of the $NaNO_3$-KNO_3-$Ca(NO_3)_2$ showed no obvious difference from those of other nitrate/nitrite systems but was still slightly higher than that of Solar Salt, Hitec XL, and the $LiNO_3$-$NaNO_3$-KNO_3. The thermal conductivity of the $NaNO_3$-KNO_3-$Ca(NO_3)_2$ eutectic salt was calculated by Equation (2), and the result is also shown in Figure 10. The obtained thermal conductivity of the sample was located in the range of 0.241–0.918 W/m·K, which can be further linearly fitted by Equation (6) from 423 K to 773 K. The adjusted R-square (R^2) was more than 99.93%. The average thermal conductivity was 0.587 $\pm$ 0.424 W/m·K at temperature ranging from 423 K to 773 K. The relatively high thermal diffusivity and thermal conductivity indicate good heat transfer properties for this salt.

$$\lambda = -5.9127 + 0.01943T \text{ (W/m·K)} \ (423 \leq T \leq 773 \text{ K}). \quad (6)$$

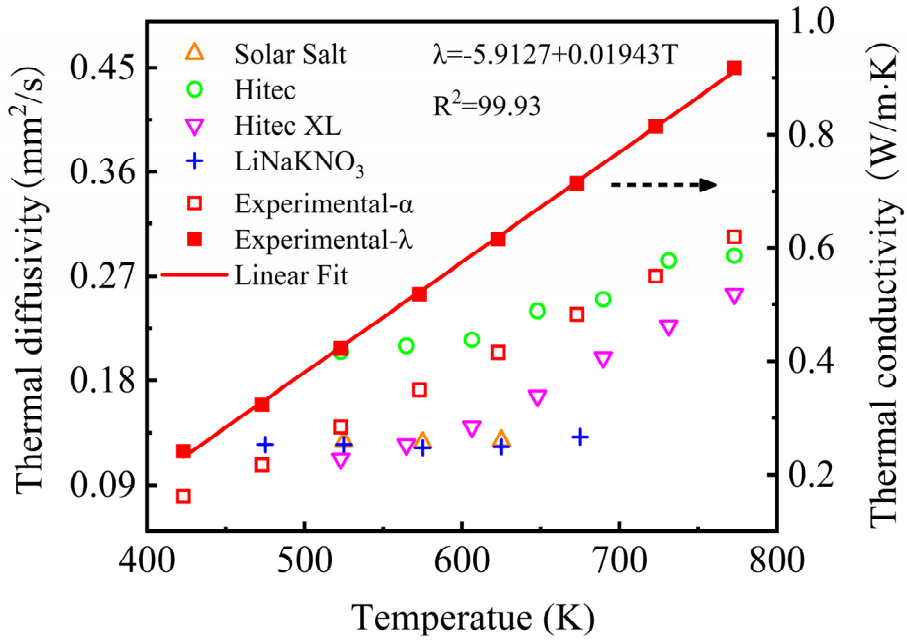

Figure 10. Thermal diffusivity of the $NaNO_3$-KNO_3-$Ca(NO_3)_2$ (16:48:36 wt%) and other currently used nitrate/nitrite systems (left *Y*-axis); the thermal conductivity of the $NaNO_3$-KNO_3-$Ca(NO_3)_2$ (16:48:36 wt%) (right *Y*-axis).

3.6. Viscosity

The viscosity of nitrate molten salt determines the flow characteristics and thermohydraulic nature of the heat exchange and storage process, which also has a significant impact on the heat exchange efficiency of the system. The viscosity of the $NaNO_3$-KNO_3-$Ca(NO_3)_2$ at different temperatures is measured and presented in Figure 11. This figure also compared the obtained experimental viscosity values of the $NaNO_3$-KNO_3-$Ca(NO_3)_2$ with that of Solar Salt, Hitec, Hitec XL, and the $LiNO_3$-$NaNO_3$-KNO_3 measured from 423 K to 773 K as reported by literature. Theoretically, the temperature dependence of viscosity is described by Arrhenius equation as shown in Equation (7), which was also adopted in this work. Regression analysis of the viscosity data with Equation (3) is also performed.

$$\eta = A_0 exp\left(\frac{E_{vis}}{RT}\right), \tag{7}$$

where A_0 is a constant, E_{vis} is the activation energy, and R is the universal gas law constant.

The result indicates that the viscosity of the $NaNO_3$-KNO_3-$Ca(NO_3)_2$ eutectic salt declined with the increase in temperature from 423 K to 773 K. The viscosity of the $NaNO_3$-KNO_3-$Ca(NO_3)_2$ ternary salt in this work ranged from 7.35 mPa·s to 1.67 mPa·s within 423 K–773 K (Figure 11), which was maintained at a relatively low level. The viscosity value of the $NaNO_3$-KNO_3-$Ca(NO_3)_2$ was significantly lower than that of Hitec XL, slightly lower than that of the $LiNO_3$-$NaNO_3$-KNO_3, and close to that of Solar Salt and Hitec in the same temperature range. The viscosity of the $NaNO_3$-KNO_3-$Ca(NO_3)_2$ can be successfully depicted by Arrhenius equation. The specific value can be fitted by an exponential function of temperature ranging from 423 K to 773 K, as expressed in Equation (8). The adjusted R-square (R^2) was more than 99.80%. The results showed that the viscosity of the studied system remained relatively low among the currently potential materials, indicating a good thermohydraulic property and satisfactory fluidity for this fluid.

$$\gamma = \exp(7.1157 - 0.0164T + 1.024510^{-5}T^2)\ (\text{mPa·s})\ (423 \leq T \leq 773\ \text{K}). \tag{8}$$

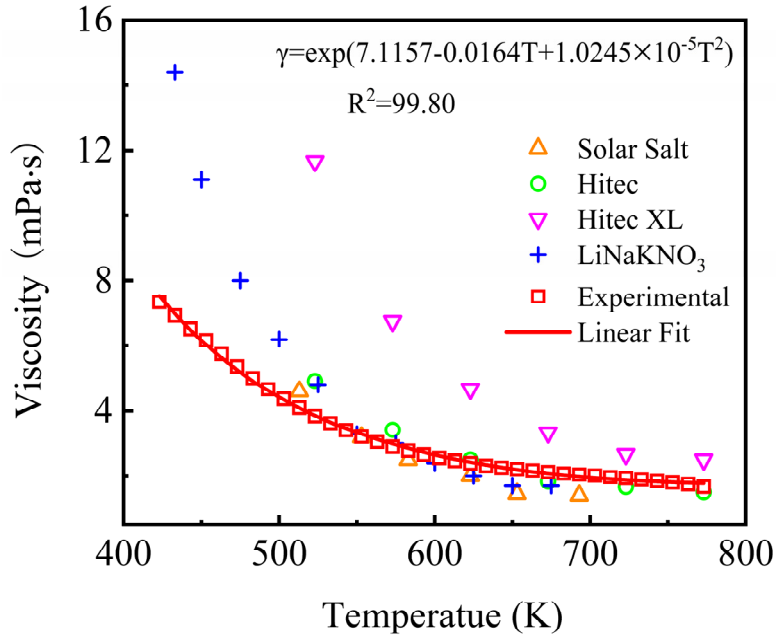

Figure 11. Viscosity of the $NaNO_3$-KNO_3-$Ca(NO_3)_2$ (16:48:36 wt%) eutectic ternary salt and other currently used nitrate/nitrite systems.

3.7. Economic Performance

The cost price of molten salt plays a significant role in evaluating the industrial scale, commercial application, and market penetration of this material. The cost price determines the development potential of a candidate TES/HTF material to some extent [43]. Therefore, the economic analysis of the target system as well as some other commonly used nitrate/nitrite salt mixtures was performed and compared in this study. The cost of a molten salt material is mainly influenced by the price of the individual salts, instrument loss and energy consumption during synthesis. However, under mass production conditions, the loss of equipment can be ignored. As for power consumption, it reached a level of 15 ¥/kg in our lab. Although this accounts for a significant portion of the cost, the power consumption is basically not much different for different molten salt materials due to their similar synthesis method. That means the price of each individual salt finally determines the cost of materials [12,44].

As mentioned above, the cost of eutectic salt mainly depends on the price of the individual salts that comprise the mixture. In the present study, the price of each individual salt was collected from the website of Sinopharm Chemical Reagent Co., Ltd. (SCRC) [45], as shown in Table 1. Notably, the salt price varies with the purity; high-purity salt indicates a high price. The salt price with a chemical purity of more than 99% is adopted in the current study. The Li-containing salt of $LiNO_3$ is the most expensive individual salt whose price is substantially higher than that of other individual salts. By contrast, $Ca(NO_3)_2$ is the cheapest one, and the single salts KNO_3, $NaNO_3$, and $NaNO_2$ with similar prices are in the middle.

Table 1. Cost price of individual salts (data from the website of Sinopharm Chemical Reagent Co., Ltd. (SCRC)).

Individual Salt	$NaNO_3$	KNO_3	$LiNO_3$	$NaNO_2$	$Ca(NO_3)_2$
Price (¥/kg)	42	46	120	40	38

With a known individual salt price, the cost of each molten nitrate/nitrite mixture was thus calculated in accordance with its specific composition. The main thermal-physical properties (T_m and T_d) and the cost price between the $NaNO_3$-KNO_3-$Ca(NO_3)_2$ and four

other current candidate nitrate/nitrite materials, namely Solar Salt, Hitec, Hitec XL, and $LiNO_3$-$NaNO_3$-KNO_3, were compared and summarized in Table 2, which is intuitively shown in Figure 12. The cost of the $NaNO_3$-KNO_3-$Ca(NO_3)_2$ salt is relatively low. Except for Hitec XL, the price of $NaNO_3$-KNO_3-$Ca(NO_3)_2$ salt is lower than others, indicating that this system has an excellent economic performance. Meanwhile, the $NaNO_3$-KNO_3-$Ca(NO_3)_2$ system has the lowest melting point of 382 K, which is the largest advantage for this system. The melting point of this system successfully decreased to 382 K, and this value is the only one below 390 K among these nitrate/nitrite mixtures. This finding is a significant improvement in the thermophysical properties of the mixed nitrate molten salts. Thus, the $NaNO_3$-KNO_3-$Ca(NO_3)_2$ system becomes a promising phase-change material (PCM) or TES/HTF material due to its aforementioned advantages. Meanwhile, this newly designed system can also be regarded as an optimized Hitec XL system with promoted properties and excellent parameters. The high-temperature thermal stability of the $NaNO_3$-KNO_3-$Ca(NO_3)_2$ has not been significantly improved; however, it is still comparable with the four other systems and remains at a relatively high level. Thus, the maximum operating temperature of 771 K for the $NaNO_3$-KNO_3-$Ca(NO_3)_2$ is also acceptable.

Table 2. Key phase change thermal-physical properties and cost of currently potential nitrate/nitrite molten salts.

Molten Salt	Composition	T_m (K)	T_d (K)	Price (¥/kg)	Ref.
Solar Salt	$NaNO_3$-KNO_3 (60-40 wt%)	513	838	43.6	[34]
Hitec	$NaNO_2$-$NaNO_3$-KNO_3 (40-7-53wt%)	415	807	43.32	[19]
Hitec XL	$NaNO_3$-KNO_3-$Ca(NO_3)_2$ (7-45-48 wt%)	400	787	41.88	[19]
$LiNaKNO_3$	$LiNO_3$-$NaNO_3$-KNO_3 (30-18-52 wt%)	397	816	67.68	[34]
$NaKCaNO_3$	$NaNO_3$-KNO_3-$Ca(NO_3)_2$ (16-48-36 wt%)	382	771	42.48	This study

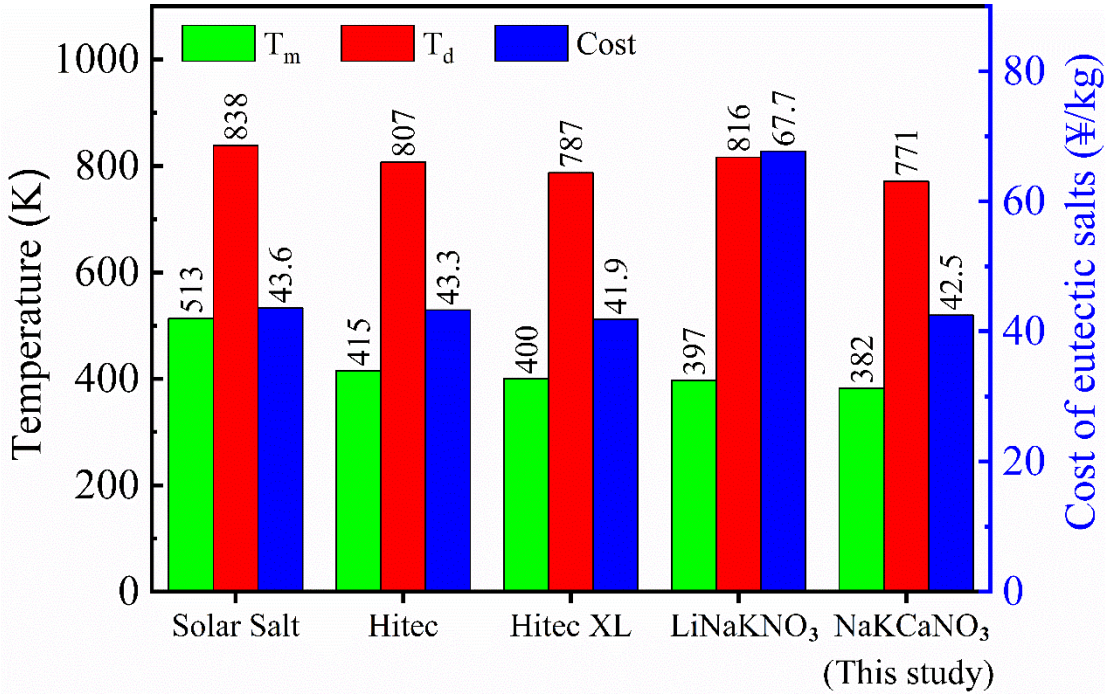

Figure 12. Melting point (T_m), decomposition temperature (T_d), and cost of the $NaNO_3$-KNO_3-$Ca(NO_3)_2$ (16:48:36 wt%) eutectic ternary salt and four other generally used nitrate/nitrite systems.

4. Discussion

4.1. Challenges and Significance of Thermophysical Properties Measurement of Molten Salts

Thermophysical properties are the key to evaluating the heat transfer and storage performances of materials. Since the measurement process of thermophysical properties for molten salt system is generally accompanied by harsh conditions such as high temperature and inert atmosphere, the testing procedure is generally time-consuming and complicated, thus resulting in a large workload. In particular, the deliquescence of molten salt samples needs to be effectively avoided during the entire sample preparation and storage and measurement process, which further increases the testing difficulty. Meanwhile, the corrosiveness of molten salts may also cause damage to equipment and container materials. In addition, the vapor of molten salt caused by volatilization can also lead to the contamination and corrosion of the experimental instrument and related accessories. All of the above issues bring challenges for molten salt measurements. Nevertheless, establishing and optimizing thermophysical data of new molten salt systems is of great practical significance for enriching the database and expanding engineering applications.

In this work, all experimental instruments were designed, modified, and manufactured according to the characteristics of high-temperature molten salt samples. Especially the densitometer and viscometer are completely self-developed instruments. Then, we comprehensively studied the thermophysical properties of the new $NaNO_3$-KNO_3-$Ca(NO_3)_2$ (16:48:36 wt%) eutectic salt by our self-developed experimental devices. The experimental results prove that our instruments can accurately obtain the thermophysical data of molten salts with good reproducibility. This work not only proposed a potential molten salt medium as TES/HTF material, but also provided its new basic thermophysical information, which enriched the engineering database for CSP system.

4.2. Advantages and Material Selection

In this study, a comparative analysis of thermal-physical properties between the studied $NaNO_3$-KNO_3-$Ca(NO_3)_2$ and other currently potential nitrate/nitrite systems that can be developed into TES/HTF materials, namely, Solar salt ($NaNO_3$-KNO_3 (60-40 wt%)), Hitec ($NaNO_2$-$NaNO_3$-KNO_3 (40-7-53 wt%)), Hitec XL ($NaNO_3$-KNO_3-$Ca(NO_3)_2$ (7-45-48 wt%)) and $LiNO_3$-$NaNO_3$-KNO_3 (30-18-52 wt%), was carried out. The results showed that the new eutectic salt has a lowest melting point (382 K), which is a great improvement and may be the biggest advantage for this system. Besides, the system also has excellent thermophysical properties and fluidity, with good heat capacity, acceptable thermal stability, favorable fusion enthalpy, wide operating temperature range, high thermal conductivity, suitable density, and low viscosity, which well meets the needs for thermal energy transfer and storage. In addition, the cost analysis also shows the system has good economic performance, indicating a competitive market penetration. All of these advantages make this salt a potential candidate material for TES/HTF. This study provides a basis for the development and selection of new molten salt materials in thermal engineering.

4.3. Applications and Prospects

We successfully designed and prepared a new $NaNO_3$-KNO_3-$Ca(NO_3)_2$ eutectic salt system with enhanced heat transfer and storage performances. Through an overall evaluation and comparative analysis, this multicomponent nitrate molten salt system was proved to have excellent thermophysical properties as well as good economic performance. Based on it, this salt was supposed to solve the problem of low efficiency of current heat storage materials, and also expected to become one of the potential TES/HTF materials for CSP applications.

Although this system has a similar composition to Hitec XL, as a newly developed multicomponent system, its overall performance has been greatly improved also with attractive cost. Therefore, it can be regarded as an optimized Hitec XL system, which broadens the application scope of nitrate systems.

However, it should be noted that the maximum operating temperature (T_d) has yet to be raised for the $NaNO_3$-KNO_3-$Ca(NO_3)_2$. In fact, most nitrates face this common problem that needs to be solved, not only just for the studied system. Herein, the T_d gap between the $NaNO_3$-KNO_3-$Ca(NO_3)_2$ and other currently potential materials is narrow (Figure 12), and the thermal stability for this system is thus considered acceptable. The high temperature thermal stability of the $NaNO_3$-KNO_3-$Ca(NO_3)_2$ eutectic salt molten salt can be regulated by adding one or more suitable molten salt additives. Relevant studies are underway in our group and some progress has been made. However, from the perspective of engineering application, a more in-depth assessment of this material is a long-term work and still to be given in the future. This work provided the basis and preliminary data for this purpose.

In summary, the present study mainly proposed a potential candidate TES/HTF material and provided a higher reference value for the development of heat transfer and storage materials in CSP applications. In addition, the newly developed nitrate salt system is also supposed to use in other high-temperature processes or thermal power generation applications, such as peak shaving of power grids, effective use of curtailed wind power, and waste heat.

5. Conclusions

In this study, a new multicomponent nitrate molten salt of the $NaNO_3$-KNO_3-$Ca(NO_3)_2$ (16:48:36 wt%) system with great improvement of lower melting temperature was successfully designed and prepared using the static fusion method. Then, its thermal-physical properties were characterized by our modified or self-developed devices. The results showed that the melting point and fusion enthalpy of the $NaNO_3$-KNO_3-$Ca(NO_3)_2$ salt were 382.1K and 57.9 J/g respectively, The weight loss of the $NaNO_3$-KNO_3-$Ca(NO_3)_2$ eutectic salt is still less than 3.0% even up to 771.1 K. The average specific heat capacity of salt in liquid state were 1.55 J/g·K. Average value of thermal conductivity and density was 0.587 W/m·K and 1.9533 g/cm^3, respectively, at the temperature range from 423 K to 773 K. The viscosity ranged from 7.35 to 1.67 mPa·s at 423–773 K. The uncertainty analysis of each measurement method was also conducted.

Furthermore, for better understanding and evaluating the heat transfer and storage performances of the material, a comparative analysis of the thermal-physical properties between the $NaNO_3$-KNO_3-$Ca(NO_3)_2$ and other currently used nitrate/nitrite systems was performed. The results proved that the $NaNO_3$-KNO_3-$Ca(NO_3)_2$ eutectic ternary system exhibits excellent thermal-physical properties with improved parameters, including low melting point, high energy storage density, good thermal conductivity, acceptable thermal stability, and wide operating temperature range. Meanwhile, the system has good flow characteristics with suitable density and relatively low viscosity. Besides, this salt also shows good economic performance with great market potential. All of these advantages make the newly developed salt a promising material for TES/HTF in CSP applications or other probable thermal power generation facilities.

Author Contributions: Conceptualization, Y.W. and H.P.; methodology, N.L. and H.P.; software, Y.W. and Q.L.; validation, H.P.; formal analysis, Q.L. and H.P.; investigation, N.L. and H.P.; resources, H.P.; data curation, H.P.; writing—original draft preparation, N.L.; writing—review and editing, H.P.; visualization, N.L. and H.P.; supervision, H.P.; project administration, H.P.; funding acquisition, H.P. All authors have read and agreed to the published version of the manuscript.

Funding: This research was funded by the National Natural Science Foundation of China (grant number 22006150) and Shanghai Sailing Program (grant number 19YF1458200). The article processing charge (APC) was funded by the Shanghai Municipal Natural Science Foundation (grant number 20ZR1464900; fund recipient: Fangling Jiang).

Institutional Review Board Statement: Not applicable.

Informed Consent Statement: Not applicable.

Data Availability Statement: Not applicable.

Conflicts of Interest: The authors declare no conflict of interest.

References

1. Alva, G.; Liu, L.; Huang, X.; Fang, G. Thermal energy storage materials and systems for solar energy applications. *Renew. Sustain. Energy Rev.* **2017**, *68*, 693–706. [CrossRef]
2. Kawanami, T.; Togashi, K.; Fumoto, K.; Hirano, S.; Zhang, P.; Shirai, K.; Hirasawa, S. Thermophysical properties and thermal characteristics of phase change emulsion for thermal energy storage media. *Energy* **2017**, *117*, 562–568. [CrossRef]
3. Pelay, U.; Luo, L.; Fan, Y.; Stitou, D.; Rood, M. Thermal energy storage systems for concentrated solar power plants. *Renew. Sustain. Energy Rev.* **2017**, *79*, 82–100. [CrossRef]
4. Cao, L.; Tang, Y.; Fang, G. Preparation and properties of shape-stabilized phase change materials based on fatty acid eutectics and cellulose composites for thermal energy storage. *Energy* **2015**, *80*, 98–103. [CrossRef]
5. Du, L.C.; Ding, J.; Tian, H.Q.; Wang, W.L.; Wei, X.L.; Song, M. Thermal properties and thermal stability of the ternary eutectic salt NaCl-CaCl2-MgCl2 used in high-temperature thermal energy storage process. *Appl. Energy* **2017**, *204*, 227–238. [CrossRef]
6. Lizana, J.; Chacartegui, R.; Barrios-Padura, A.; Valverde, J.M. Advances in thermal energy storage materials and their applications towards zero energy buildings: A critical review. *Appl. Energy* **2017**, *203*, 219–239. [CrossRef]
7. Gulfam, R.; Zhang, P.; Meng, Z. Advanced thermal systems driven by paraffin-based phase change materials—A review. *Appl. Energy* **2019**, *238*, 582–611. [CrossRef]
8. Wang, T.; Mantha, D.; Reddy, R.G. Novel low melting point quaternary eutectic system for solar thermal energy storage. *Appl. Energy* **2013**, *102*, 1422–1429. [CrossRef]
9. Bonk, A.; Sau, S.; Uranga, N.; Hernaiz, M.; Bauer, T. Advanced heat transfer fluids for direct molten salt line-focusing CSP plants. *Prog. Energy Combust. Sci.* **2018**, *67*, 69–87. [CrossRef]
10. Prasher, H.R. The prospect of high temperature solid state energy conversion to reduce the cost of concentrated solar power. *Energy Environ. Sci.* **2014**, *7*, 1819–1828.
11. Li, X.; Wang, Y.; Wu, S.; Xie, L. Preparation and investigation of multicomponent alkali nitrate/nitrite salts for low temperature thermal energy storage. *Energy* **2018**, *160*, 1021–1029. [CrossRef]
12. Wu, S.; Peng, H.; Ao, J.; Xie, L. Design and development of novel LiCl–NaCl–KCl–ZnCl2 eutectic chlorides for thermal storage fluids in concentrating solar power (CSP) applications. *Sol. Energy Mater. Sol. Cells* **2022**, *240*, 111678. [CrossRef]
13. Janz, G.J.; Truong, G.N. Melting and premelting properties of the potassium nitrate-sodium nitrite-sodium nitrate eutectic system. *J. Chem. Eng. Data* **1983**, *28*, 201–202. [CrossRef]
14. Villada, F.; Jaramillo, J.G.; Castano, F.; Echeverria, F.; Bolivar, F. Design and development of nitrate-nitrite based molten salts for concentrating solar power applications. *Sol. Energy* **2019**, *188*, 291–299. [CrossRef]
15. Medrano, M.; Gil, A.; Martorell, I.; Potau, X.; Cabeza, L.F. State of the art on high-temperature thermal energy storage for power generation. Part 2—Case studies. *Renew. Sustain. Energy Rev.* **2010**, *14*, 56–72. [CrossRef]
16. Roget, F.; Favotto, C.; Rogez, J. Study of the KNO3–LiNO3 and KNO3–NaNO3–LiNO3 eutectics as phase change materials for thermal storage in a low-temperature solar power plant. *Sol. Energy* **2013**, *95*, 155–169. [CrossRef]
17. Henríquez, M.; Guerreiro, L.; Fernández, G.; Fuentealba, E. Lithium nitrate purity influence assessment in ternary molten salts as thermal energy storage material for CSP plants. *Renew. Energy* **2020**, *149*, 940–950. [CrossRef]
18. Gil, A.; Medrano, M.; Martorell, I.; Lázaro, A.; Dolado, P.; Zalba, B.; Cabeza, L.F. State of the art on high temperature thermal energy storage for power generation. Part 1—Concepts, materials and modellization. *Renew. Sustain. Energy Rev.* **2010**, *14*, 31–55. [CrossRef]
19. Han, Y.; Yuting, W.U.; Chongfang, M.A. Comparative analysis of thermophysical properties of mixed nitrates. *Energy Storage Sci. Technol.* **2019**, *8*, 1224–1229.
20. Myers, P.D.; Goswami, D.Y. Thermal energy storage using chloride salts and their eutectics. *Appl. Therm. Eng.* **2016**, *109*, 889–900. [CrossRef]
21. Vignarooban, K.; Xu, X.; Arvay, A.; Hsu, K.; Kannan, A. Heat transfer fluids for concentrating solar power systems—A review. *Appl. Energy* **2015**, *146*, 383–396. [CrossRef]
22. Mohan, G.; Venkataraman, M.B.; Coventry, J. Sensible energy storage options for concentrating solar power plants operating above 600 °C. *Renew. Sustain. Energy Rev.* **2019**, *107*, 319–337. [CrossRef]
23. Ding, W.; Gomez-Vidal, J.; Bonk, A.; Bauer, T. Molten chloride salts for next generation CSP plants: Electrolytical salt purification for reducing corrosive impurity level. *Sol. Energy Mater. Sol. Cells* **2019**, *199*, 8–15. [CrossRef]
24. Zhou, S.K.; Wu, S. Medium and high-temperature latent heat thermal energy storage: Material database, system review, and corrosivity assessment. *Int. J. Energ. Res.* **2019**, *43*, 621–661. [CrossRef]
25. Guo, L.L.; Liu, Q.; Yin, H.Q.; Pan, T.J.; Tang, Z.F. Excellent corrosion resistance of 316 stainless steel in purified NaCl-$MgCl_2$ eutectic salt at high temperature. *Corros. Sci.* **2020**, *166*, 108473. [CrossRef]
26. Mohan, G.; Venkataraman, M.; Gomez-Vidal, J.; Coventry, J. Thermo-economic analysis of high-temperature sensible thermal storage with different ternary eutectic alkali and alkaline earth metal chlorides. *Sol. Energy* **2018**, *176*, 350–357. [CrossRef]
27. Mehos, M.; Turchi, C.; Vidal, J.; Wagner, M.; Ma, Z.; Ho, C.; Kolb, W.; Andraka, C.; Kruizenga, A. *Concentrating Solar Power Gen 3 Demonstration Roadmap*; Technical Report NREL/TP; Office of Scientific and Technical Information (OSTI): Oak Ridge, TN, USA, 2017; pp. 5500–67464.

28. Fernández, A.G.; Gomez-Vidal, J.; Oró, E.; Kruizenga, A.; Solé, A.; Cabeza, L.F. Mainstreaming commercial CSP systems: A technology review. *Renew. Energy* **2019**, *140*, 152–176. [CrossRef]
29. Margolis, R.; Coggeshall, C.; Zuboy, J. *Sunshot Vision Study*; US Department of Energy: Washington, DC, USA, 2012.
30. Vignarooban, K.; Pugazhendhi, P.; Tucker, C.; Gervasio, D.; Kannan, A. Corrosion resistance of Hastelloys in molten metal-chloride heat-transfer fluids for concentrating solar power applications. *Sol. Energy* **2014**, *103*, 62–69. [CrossRef]
31. Ding, W.; Bonk, A.; Bauer, T. Corrosion behavior of metallic alloys in molten chloride salts for thermal energy storage in concentrated solar power plants: A review. *Front. Chem. Sci. Eng.* **2018**, *12*, 564–576. [CrossRef]
32. Gaune-Escard, M.; Haarberg, G.M. *Mohen Salts Chemistry and Technology*; John Wiley & Sons, Ltd: Chichester, UK, 2014; pp. 543–553.
33. Gomez, J.C.; Calvet, N.; Starace, A.K.; Glatzmaier, G.C. $Ca(NO_3)_2$-$NaNO_3$-KNO_3 molten salt mixtures for direct thermal energy storage systems in parabolic trough plants. *J. Sol. Energy Eng.* **2013**, *135*, 0210161–0210168. [CrossRef]
34. Zhang, P.; Cheng, J.; Jin, Y.; An, X. Evaluation of thermal physical properties of molten nitrate salts with low melting temperature. *Sol. Energy Mater. Sol. Cells* **2018**, *176*, 36–41. [CrossRef]
35. *ASTM 1269-11*; Standard Test Method for Determining Specific Heat Capacity by Differential Scanning Calorimetry. ASTM International: West Conshohocken, PA, USA, 2018.
36. Cheng, J.-H.; Zhang, P.; An, X.-H.; Wang, K.; Zuo, Y.; Yan, H.-W.; Li, Z.; Jin-Hui, C.; Peng, Z.; Xue-Hui, A.; et al. A Device for Measuring the Density and Liquidus Temperature of Molten Fluorides for Heat Transfer and Storage. *Chin. Phys. Lett.* **2013**, *30*, 126501. [CrossRef]
37. An, X.-H.; Cheng, J.-H.; Yin, H.-Q.; Xie, L.-D.; Zhang, P. Thermal conductivity of high temperature fluoride molten salt determined by laser flash technique. *Int. J. Heat Mass Transf.* **2015**, *90*, 872–877. [CrossRef]
38. Janz, G.J.; Krebs, U.; Siegenthaler, H.F.; Tomkins, R.P.T. Molten salts: Volume 3, nitrates, nitrites and mixtures-electrical conductance, density, viscosity and surface tension data. *J. Phys. Chem. Ref. Data* **1973**, *1*, 582–746. [CrossRef]
39. Jin, Y.; Cheng, J.; An, X.; Su, T.; Zhang, P.; Li, Z. Accurate viscosity measurement of nitrates/nitrites salts for concentrated solar power. *Sol. Energy* **2016**, *137*, 385–392. [CrossRef]
40. Elfeky, K.E.; Ahmed, N.; Naqvi, S.M.A.; Wang, Q. Numerical comparison between single PCM and multi-stage PCM based high temperature thermal energy storage for CSP tower plants. *Appl. Therm. Eng.* **2018**, *139*, 609–622. [CrossRef]
41. Elfeky, K.; Li, X.; Ahmed, N.; Lu, L.; Wang, Q. Optimization of thermal performance in thermocline tank thermal energy storage system with the multilayered PCM(s) for CSP tower plants. *Appl. Energy* **2019**, *243*, 175–190. [CrossRef]
42. Chen, Y.; Zhao, C. Thermophysical properties of Ca(NO3)2-NaNO3-KNO3 mixtures for heat transfer and thermal storage. *Sol. Energy* **2017**, *146*, 172–179. [CrossRef]
43. Kim, H.; Yoon, S.H.; Kim, Y.; Lee, K.H.; Choi, J.S. Experimental studies on the charging performance of single-tank single-mediumthermal energy storage. *Appl. Therm. Eng.* **2019**, *149*, 1098–1104. [CrossRef]
44. Wang, Y.; Li, X.; Li, N.; Ling, C.; Tang, Z.; Li, Z. Thermal transport and storage performances of NaCl–KCl–NaF eutectic salt for high temperatures latent heat. *Sol. Energy Mater. Sol. Cells* **2020**, *218*, 110756. [CrossRef]
45. Sinopharm Chemical Reagent. Available online: https://www.sinoreagent.com/ (accessed on 1 January 2019).